Full Paper Transactions, SMiRT 28
Toronto, Canada, August 10-15, 2025

EFFECT OF LOCAL SOIL PLASTICITY ON THE SEISMIC RESPONSE OF NUCLEAR STRUCTURES IN SSI ANALYSIS USING THE DOMAIN REDUCTION METHOD

Jan Attinger[1], Miriam Kleinhenz[2], Tadeusz Szczesiak[3], Sara Ghadimi Khasraghy[4], Peter Rangelow[5], Yves Mondet[6]

[1] Project Leader, Basler & Hofmann AG, Zurich, Switzerland (Jan.Attinger@baslerhofmann.ch)
[2] Dr., Structural Engineer, Basler & Hofmann AG, Zurich, Switzerland
[3] Dr., Deputy Section Head of Civil Engineering, Swiss Federal Nuclear Safety Inspectorate ENSI, Brugg, Switzerland
[4] Dr., Civil Engineering Specialist, Swiss Federal Nuclear Safety Inspectorate ENSI, Brugg, Switzerland
[5] Dr., Senior Expert, Basler & Hofmann AG, Zurich, Switzerland
[6] Head of Section Structural Safety, Basler & Hofmann AG, Zurich, Switzerland

ABSTRACT

To comply with the updated ENSI-2015 seismic hazard assessment, Swiss nuclear power plant (NPP) operators were required to revise their seismic safety evaluations. A critical aspect is the consideration of Soil-Structure Interaction (SSI) in structural safety assessment and In-Structure Response Spectra (ISRS) calculations.

This study is based on the findings of Attinger et al. (2024), who examined the effects of sliding and uplifting of a reactor building on the ISRS using the Domain Reduction Method (DRM) with linear material models and nonlinear structure-soil interface (Run 2) in comparison to the linear reference analysis (Run 1). The current study extends the previous analyses to include also soil plasticity under the foundation (Run 3) during a Safe Shutdown Earthquake (SSE). A kinematic hardening soil model is implemented to capture the nonlinear soil behaviour.

The results indicate that soil plasticity primarily affects the fundamental rocking mode, reducing the maximum spectral acceleration by up to 30% compared to the linear reference analysis and 15% compared to the analysis with nonlinear structure-soil interface, while vertical and horizontal spectral accelerations near the foundation remain less affected, with occasional increases. Peak displacements remain relatively constant across linear and both nonlinear analyses. However, small permanent tangential displacements are observed for the frictional contact between soil and building, which cannot be attributed to global sliding but are likely induced by the three-dimensional input motion. These displacements are expected to be significantly reduced when considering a more realistic modelling of the reactor building embedment, suggesting that potential impacts on pipes entering the reactor building are unlikely.

INTRODUCTION

The updated seismic hazard ENSI-2015 has increased significantly compared to the original design basis. Consequently, Swiss NPP operators were required to update their seismic safety assessment, including the In-Structure-Response-Spectra (ISRS).

For higher-intensity seismic excitations, conventional linear methods that neglect non-linear contact and soil behaviour may no longer be suitable for the computation of ISRS. Since ISRS play a crucial role in assessing the safety of Structures, Systems, and Components (SSC), a deeper understanding of the transition from linear to nonlinear soil-structure interaction behaviour is essential. The Domain Reduction

Method (DRM) has emerged as a state-of-the-art approach for addressing nonlinear SSI problems and is used in this paper.

OBJECTIVE AND SCOPE

Based on the previous study that examined the influence of contact uplift and sliding (Attinger et al. 2024), this paper investigates the additional influence of local soil plasticity on the seismic response of nuclear structures. Understanding the extent to which soil plasticity affects the seismic response is essential for higher-intensity seismic excitations.

FINITE ELEMENT MODEL

The finite element (FE) model of a NPP was introduced in a previous study (Attinger et al. 2024). The simplified reactor building model features a diameter of 42 m, a height of 70 m, and a total weight of 480 MN. The internal structure, including key components such as the steel containment, polar crane, shield wall, reactor pressure vessel, and drywell, is represented by a stick model composed of beam elements and lumped masses. These beam elements are connected to the basemat perimeter by eight radially arranged, equally spaced rigid connector beams. The concrete containment is modelled using shell elements in ANSYS.

The interior soil domain measures 30 × 91 × 91 m³, as illustrated in Figure 1. Bottom nodes at the outer boundary of the computational domain are fixed, while the side nodes are coupled to Lysmer-Kuhlemeyer dampers to absorb outgoing waves and simulate proper radiation damping. The soil stiffness and damping properties replicate typical conditions at a Central European NPP site, with a moderately stiff soil layer (mean shear wave velocity $v_s \approx 500$ m/s) extending to a depth of 18 m, underlain by a significantly stiffer layer with v_s exceeding 800 m/s.

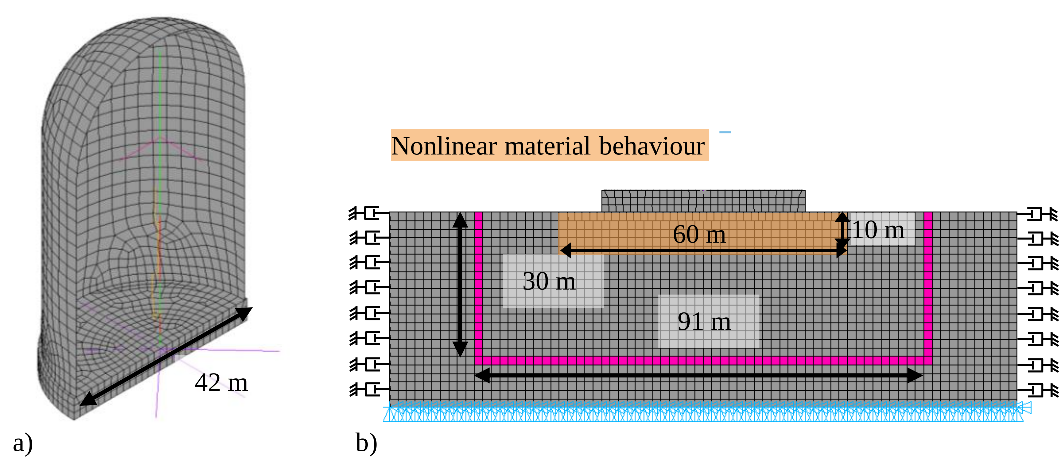

Figure 1. Ansys model: a) Reactor; b) Soil domain with soil elements under the foundation with nonlinear material behaviour.

A friction coefficient of μ = 0.8 between the basemat and the soil is used for the interface nonlinearities such as uplift and sliding. The analyses use a 5-millisecond time-step for the transient analyses. The gravity load is applied in a preliminary static analysis step. In the subsequent transient analysis, the seismic motion is induced via effective seismic forces at the nodes of the DRM elements (magenta in Figure 1). The effective forces were calculated beforehand with a Real-ESSI module (Jeremić, B. et al., 2020).

IMPLEMENTATION OF THE KINEMATIC HARDENING SOIL MODEL

In a general three-dimensional stress state, the von Mises stress is numerically equal to the deviatoric stress invariant q and is commonly used to predict yielding:

$$\sigma_v = q = \sqrt{\frac{1}{2}[(\sigma_1 - \sigma_2)^2 + (\sigma_2 - \sigma_3)^2 + (\sigma_3 - \sigma_1)^2]}$$

For uniaxial loading, where $\sigma_2 = \sigma_3 = 0$, the deviatoric stress simplifies to $q = \sigma_1$, indicating that the uniaxial yield stress defines the yield surface in three dimensions, i.e., $q_\mathrm{y} = \sigma_\mathrm{y}$.

In horizontally layered soils, where the horizontal stresses are assumed to be equal ($\sigma_2 = \sigma_3$), the yield deviatoric stress simplifies to:

$$q_\mathrm{y} = \sigma_{1,\mathrm{max}} - \sigma_3 \tag{1}$$

Unlike in steel, where yielding is governed by a single parameter (the uniaxial tensile yield strength), soil yielding depends on both the friction angle and the mean (hydrostatic) stress. By assuming constant horizontal stresses in a soil element, the yield stress can be calibrated accordingly.

The stress state of the reference soil element at a depth of 15 m is computed using the material properties listed in Table 1. The vertical stress σ_1 and the horizontal stress σ_3 are therefore:

$$\sigma_1 = \gamma \cdot h = 20 \text{ kN/m}^3 \cdot 15 \text{ m} = 300 \text{ kN/m}^2 \tag{2}$$

$$\sigma_3 = \sigma_1 \cdot K_0 = 300 \text{ kN/m}^2 \cdot 0.5 = 150 \text{ kN/m}^2 \tag{3}$$

where K_0 is the coefficient of earth pressure at rest, γ is the soil's unit weight, and h is the overburden depth.

Table 1: Material parameters of the soil elements under the foundation (gravel sand).

Initial Stiffness	E_0	1 000 000 kN/m^2
Assumed Post-yielding Stiffness	E_{post}	E_0 / 5 = 200 000 kN/m^2
Soil's Unit Weight	γ	20 kN/m^3
Friction Angle	φ	30°
Cohesion	c	0 kN/m^2
Coefficient of Earth Pressure at Rest	K_0	0.5

Using the Mohr-Coulomb yield criterion (a standard assumption for soils) and assuming constant horizontal stresses, the maximum vertical stress $\sigma_{1,\mathrm{max}}$ is determined to be 450 kN/m^2. The deviatoric yield stress is then defined as $q_\mathrm{y} = 300\ kN/m^2$, as shown in Figure 2.

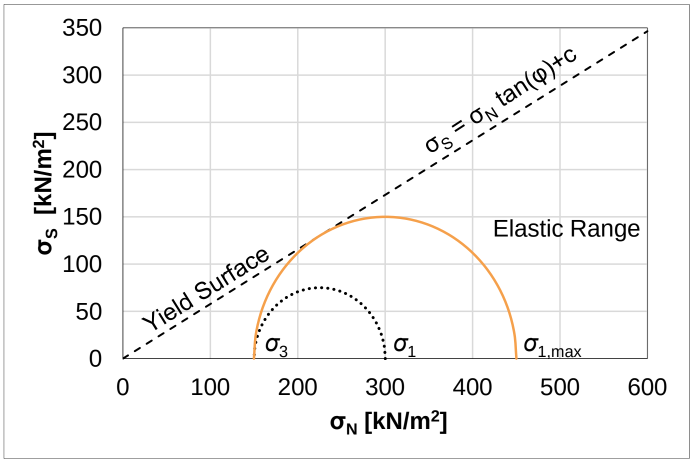

Figure 2. Mohr-Coloumb yield criterion based on the material parameters, as shown in Table 1.

The soil elements, in which bilinear kinematic behaviour is applied, span dimensions of $10 \times 60 \times 60$ m^3, as shown in Figure 1. An additional 10 m of soil overburden, which was assumed for the yield criterion, is not included in the FE-model. The backbone curve and the hysteretic stress-strain path of the kinematic hardening model are illustrated in Figure 3. The post-yielding stiffness is assumed to be one-fifth of the initial stiffness, $E_{\text{post}} = \frac{1}{5} E_0$. This is a reasonable assumption for this type of soil (Lang et al. 2011).

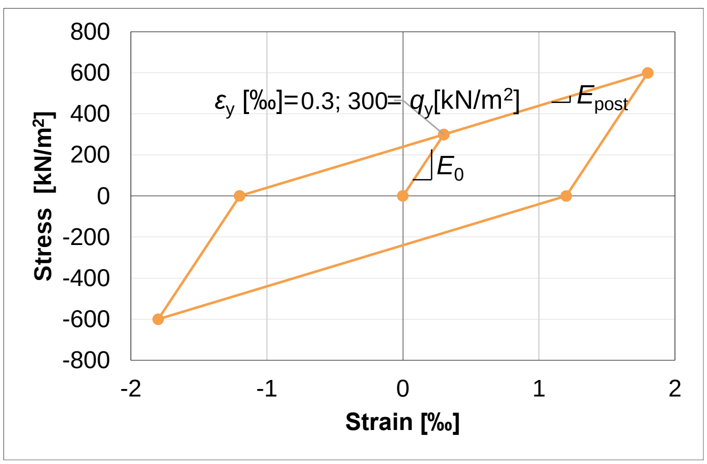

Figure 3. Bilinear kinematic hardening model.

RESULTS

To investigate the effects of the local soil plasticity on the reactor building's response, a three-dimensional SSE ground motion with a peak horizontal ground acceleration (PGA) of 0.35 g was applied. Table 2 provides an overview of the model runs (see Figure 4) and the key settings.

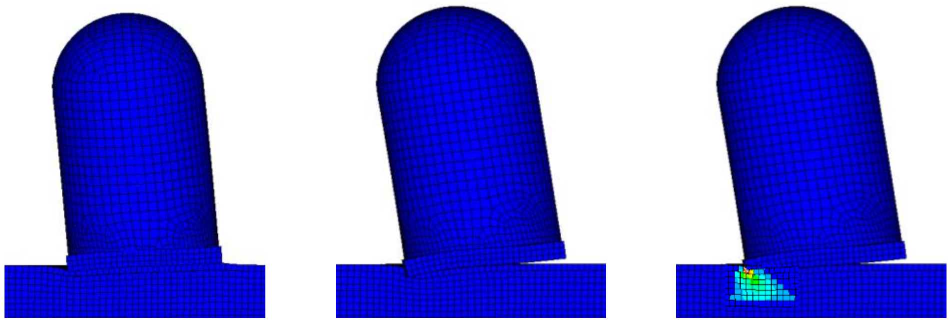

a) b) c)

Figure 4. ANSYS analyses: a) Linear Contact; b) Nonlinear Contact; c) Nonlinear Contact & Soil.

Table 2: ANSYS analyses.

Run	SSE	Foundation Contact	Local Soil Plasticity
1	**Linear Contact**[1]	Bonded Contact (linear)	Linear Elastic Behaviour
2	**Nonlinear Contact**[1]	Frictional Contact (nonlinear)	Linear Elastic Behaviour
3	**Nonlinear Contact & Soil**	Frictional Contact (nonlinear)	Bilinear Elastic-Plastic Behaviour
[1] Results taken from Attinger et al. (2024).			

Effects of the local soil plasticity

For the analysis including nonlinear contact and plastic soil behaviour (Run 3), Figure 5 shows the plastic von Mises strains ε_{pl} in the soil at three time steps of the transient analyses (after applying the dead load): the initial state of the (t = 0.0 s), the moment of maximum eccentricity (t = 4.9 s), and the final time step (t = 10.0 s). The results show that plastic strains are concentrated near the foundation edges and progressively increase over the seismic loading cycles. The plastic von Mises strains reach a maximum value of 2.8 ‰.

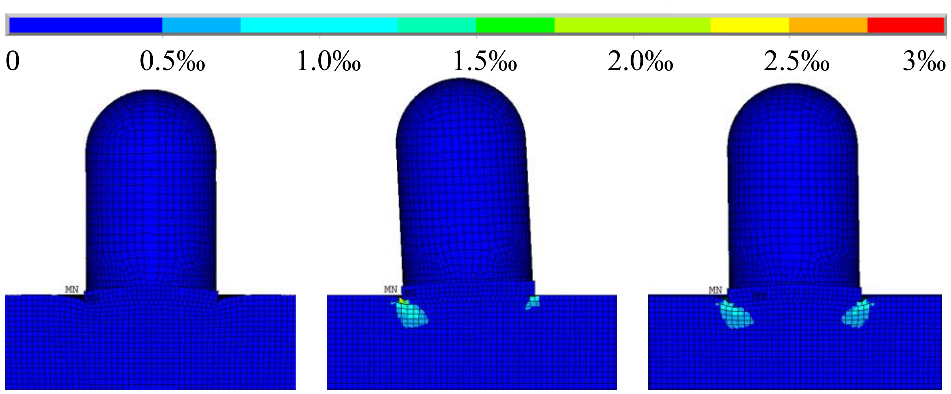

a) b) c)

Figure 5. Plastic von Mises strains [‰] at different time steps of the transient analyses: a) at t = 0.0 s; b) at t = 4.9 s; c) at t = 10 s

Base Moment and base Shear

To better understand the global reaction forces at the foundation-soil interface, Figure 6 shows the base moments around the X-axis (M_x) and Figure 7 shows the shear force and activated friction at the base for the three runs. The peak values are nearly identical between Run 2 and 3. In Run 3, which includes additional soil plasticity, the reaction moments are reduced by up to 20% compared to the linear reference analysis (Run 1).

In addition to the base moments, Figure 6 also shows the eccentricity $e = M_{res} / F_z$ normalized to the reactor building radius (r = 21 m), where the resulting moment is $M_{res} = (M_x^2 + M_y^2)^{0.5}$ and the vertical force is denoted as F_z. For the SSE with linear elastic soil material behaviour, the maximum eccentricity reaches 16.1 m for Run 1 and 10.5 m for Run 2, corresponding to normalized eccentricities e/r of 0.77 and 0.50, respectively. With soil plasticity (Run 3), the maximum eccentricity further decreases further to 8.9 m, resulting in a normalized eccentricity of 0.42. The fact that the maximum eccentricity remains well within the foundation area confirms the overall stability of the reactor building.

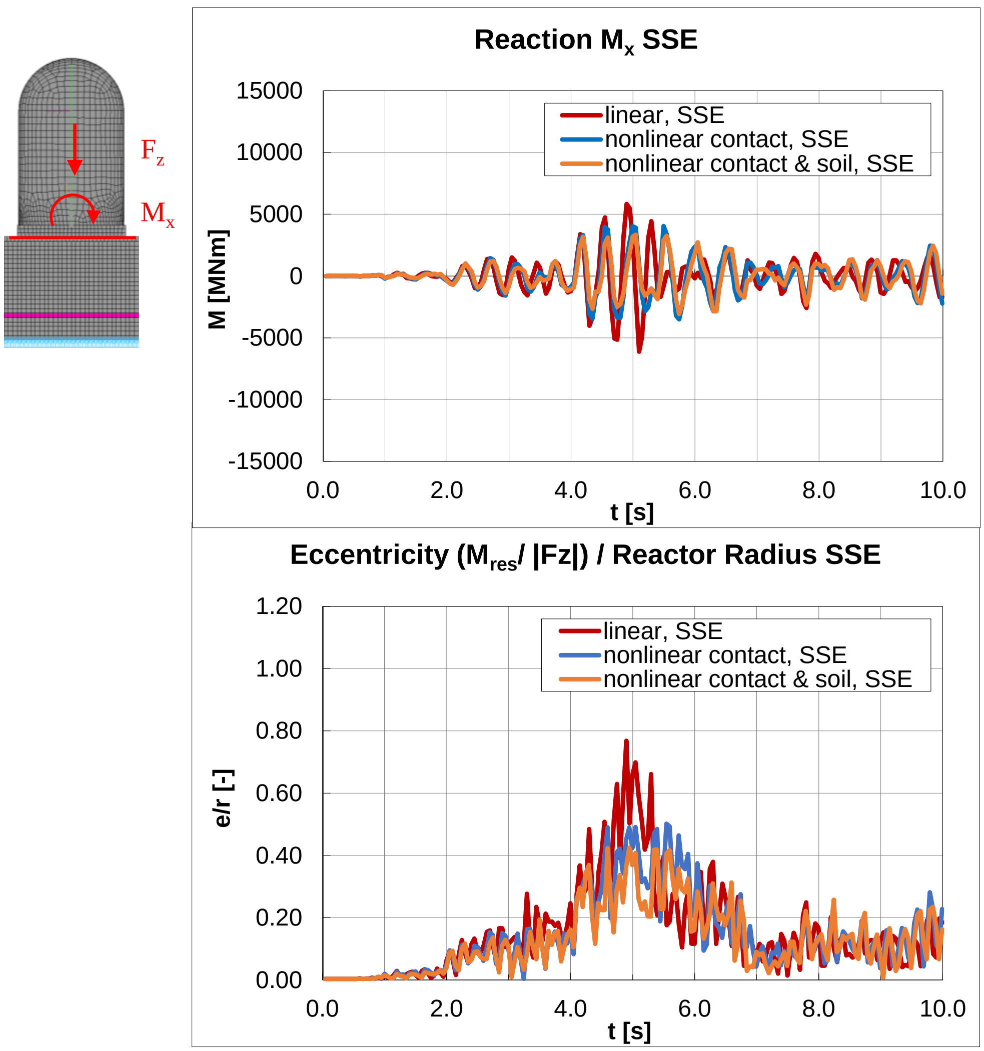

Figure 6. Comparison of the base moment reactions: moments and eccentricities.

Figure 7 shows the base shear force V and activated friction μ at the base for the three runs. The peaks are almost identical between Run 2 and 3. Since the activated friction remains below the assumed threshold of μ = 0.8, global sliding is not expected.

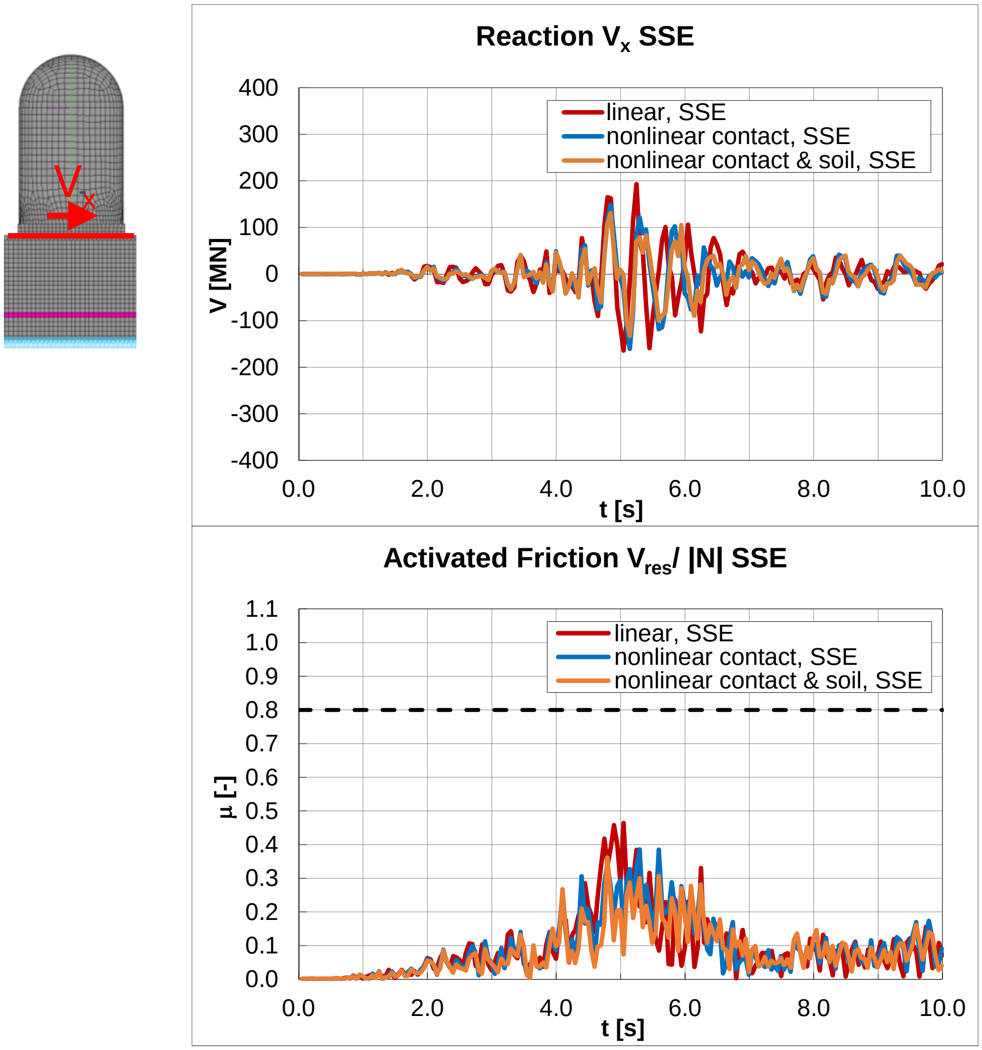

Figure 7. Comparison of the base shear reactions: shear forces and frictions.

In-Structure Response Spectra (ISRS)

Figure 8 shows a comparison of ISRS for the top nodes of both the concrete and the steel containment structures. These nodes are located along the central axis of the reactor building at heights of 69.5 m (top of concrete containment) and 67.2 m (top of steel containment) above the ground surface, respectively. For both nodes, the fundamental rocking mode is clearly observed between 2 and 3 Hz. The results indicate a monotonic decrease in peak spectral accelerations of the first mode as the model progresses from linear (Run 1) to contact non-linear (Run 2) and then to contact and soil non-linear (Run 3).The spectral acceleration of the fundamental mode decreases between Run 1 and Run 2 by approximately 15%, between Run 1 and Run 3 by approximately 30%.

For the second mode of the steel containment, the spectral acceleration initially increases from Run 1 to Run 2. This behaviour is likely due to impact effects associated with uplift, which excite a mode near 10 Hz in the steel containment. However, in Run 3, the peak spectral acceleration of the second mode falls below the Run 1 value. A plausible explanation for this behaviour is that, when soil plasticity is considered (Run 3), the impact following uplift leads to lower forces compared to the elastic soil case (Run 2). As a result, the excitation of this mode is significantly reduced in the presence of plastic soil behaviour.

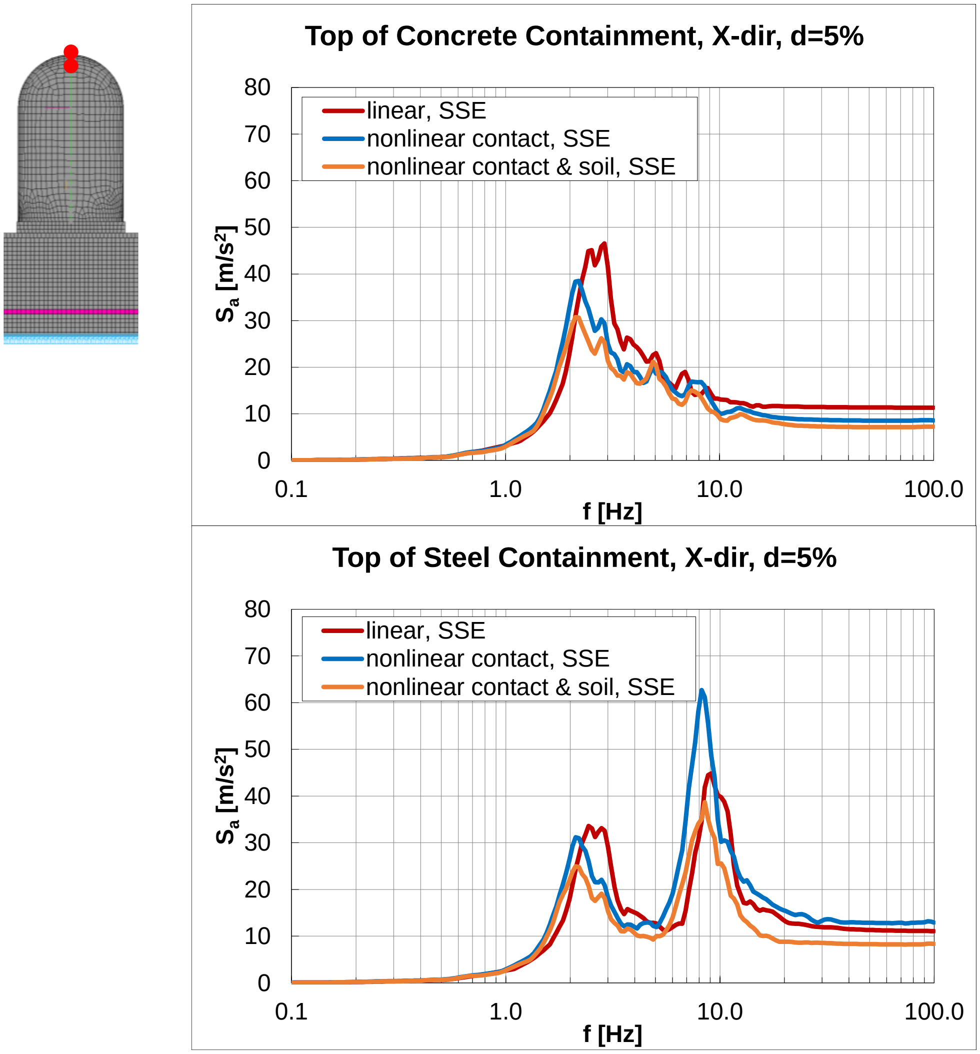

Figure 8. ISRS for SSE at the top of concrete containment and steel containment.

Relative Displacements

Figure 9 shows the relative displacement of a node located on the circumference of the concrete containment, approximately 28 m above the ground surface, which corresponds to the roof level of the surrounding auxiliary buildings. Unlike the accelerations where a reduction of the peak values is observed as non-linear effects are introduced, the peak radial displacements (Δ_{ur}) remain almost identical across all three Runs.

For the tangential displacements (Δ_{ut}), permanent displacements were observed in the non-linear analysis (Run 2 and 3). The permanent displacement decreases from approximately 2 cm to 1 cm between Run 2 and Run 3.

It is important to note that these displacements are not caused by global sliding, as the ratio of base shear force to base normal force never exceeds the friction threshold of $\mu = 0.8$. Instead, they are likely induced by the three-dimensional input motion. When the building tilts to one side while experiencing a perpendicular force, it can generate a rotational motion in the structure.

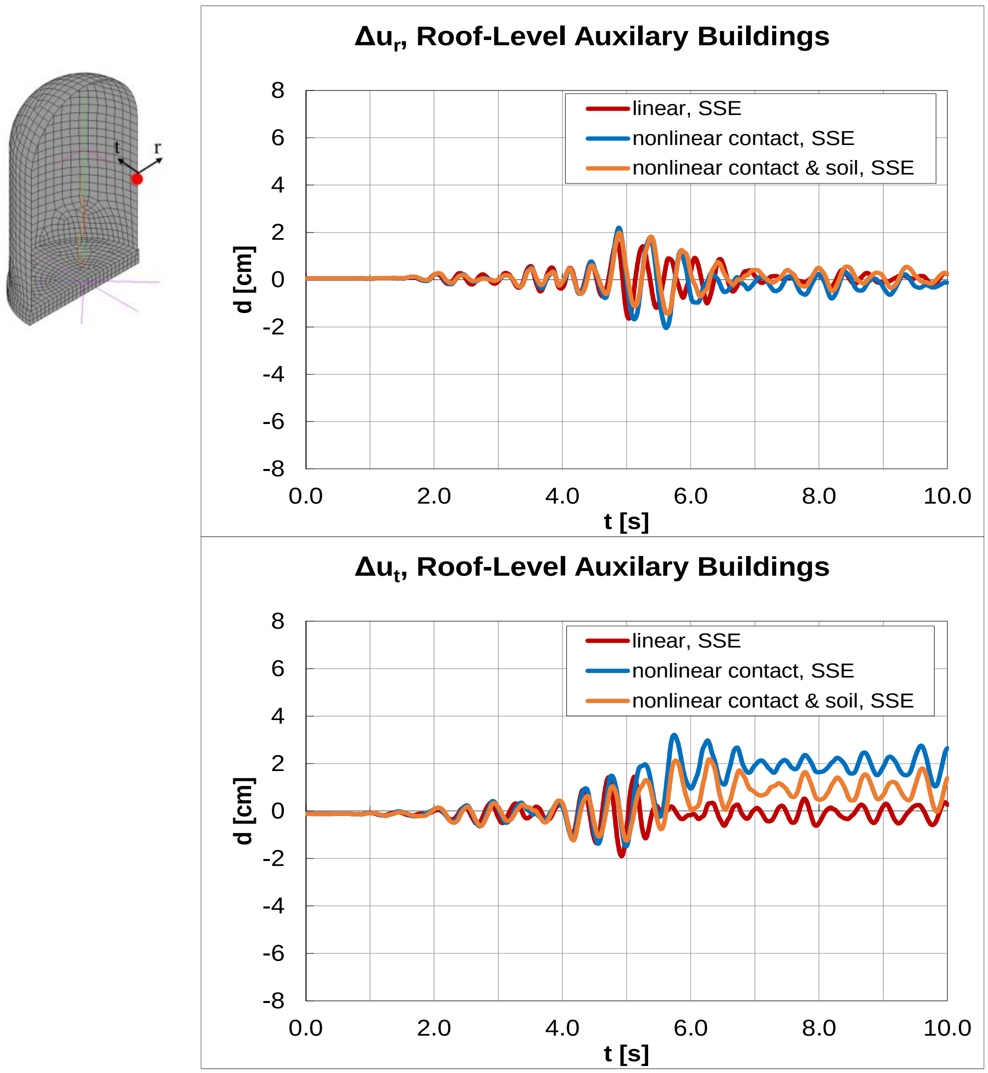

Figure 9. Relative displacements at the circumference of the concrete containment of the reactor building at the roof level of the auxiliary buildings.

CONCLUSIONS AND OUTLOOK

The yielding zone in the soil primarily develops along the foundation edge of the reactor building and expands with increasing seismic load cycles. Based on the current study, the introduction of soil plasticity in the FE-model significantly decreases the fundamental rocking mode, with a reduction of the spectral acceleration up to 30% compared to the linear reference analysis. In contrast, horizontal responses near the foundation and vertical responses remain less affected.

At the potential pounding location between the reactor building and the auxiliary buildings, radial displacements are nearly identical across all runs. However, small tangential displacements of the circumference nodes are observed, which cannot be attributed to global sliding but are probably induced by the three-dimensional input motion. For Run 3, the permanent tangential displacement reaches approximately 1 cm. However, this value is expected to decrease when the foundation's effective embedment is considered.

Future research will focus on refining the soil plasticity model, introducing the embedment of the building, and investigating beyond-design earthquake excitations to further verify the findings of this case study.

REFERENCES

ANSYS Inc. (2021), ANSYS Software Version 2021 R2, *Theoretical Manuals.*

Attinger, J., De Maddalena, C., Zimos, D., Szczesiak, T., Ghadimi, S., Rangelow, P., Mondet, Y. (2024). "Effect of Foundation Uplift and Sliding on the Seismic Response of Nuclear Structures in SSI Analysis using the Domain Reduction Method*", Transactions of the SMiRT-27*, Yokohama, Japan.

Jeremić, B. et al. (2020). *Nonlinear Finite Elements: Modeling and Simulation of Earthquakes, Soils, Structures and their Interaction*. UC Davis and LBNL, CA, USA. ISBN:978-0-692-19875-9 Real-ESSI Simulator: sokocalo.engr.ucdavis.edu/~jeremic/Real_ESSI_Simulator/

Lang, et al. (2011) *Bodenmechanik und grundbau*. Springer Berlin Heidelberg

Proseis AG (2015). "Calculation of the Seismic Hazard at the Four NPP Sites Based on the Hybrid SED-PRP Model*", Report for ENSI, PS-TA-1587*, Zurich, Switzerland.

Zimos, D., De Maddalena, C., Szczesiak, T., Rangelow, P. Mondet, Y. (2022*)*. "SSI-Analysis of Nuclear Structures in the Time-Domain using Real-ESSI". *SMiRT-26*, Berlin.